



## Note

Chiral induction based on carbohydrate ligands in olefin  
platinum(0) complexesCristina De Castro,<sup>a</sup> Antonio Molinaro,<sup>a,\*</sup> Federico Giordano,<sup>b</sup> Ida Orabona,<sup>b</sup>  
Francesco Ruffo<sup>b,\*</sup><sup>a</sup>*Dipartimento di Chimica Organica e Biochimica, Università di Napoli Federico II, Complesso Universitario Monte S. Angelo, via Cintia,  
I-80126 Napoli, Italy*<sup>b</sup>*Dipartimento di Chimica, Università di Napoli Federico II, Complesso Universitario Monte S. Angelo, via Cintia, I-80126 Napoli, Italy*

Received 8 November 2001; received in revised form 2 January 2002; accepted 6 February 2002

## Abstract

A chiral N,N-ligand based on glucose is able to recognise selectively one enantioface of a prochiral olefin in a trigonal Pt environment. NMR and X-ray studies have been carried out aiming to disclose the factors, which govern this unexpected result. The selectivity originates from the ability of the ligand to create a chiral pocket of  $C_2$  symmetry, which is retained in both solution and solid state. © 2002 Elsevier Science Ltd. All rights reserved.

**Keywords:** Platinum; Carbohydrate; NMR; Olefin-coordination; Crystal structure

The capability to achieve a metal-assisted asymmetric process relies on the careful choice of chiral ancillary ligands. A fundamental prerequisite is the creation of a chiral pocket around the metal, which must be rigid and configurationally stable. In most cases, the enantioselectivity originates from the different steric interactions that the two enantiofaces of a prochiral substrate experience within the asymmetric environment. This discrimination can influence either thermodynamics or kinetics of the process. For example, the enantiomeric excess in allylic alkylations catalysed by Pd is thought to be governed by steric intramolecular contacts which affect the relative stabilities of diastereomeric trigonal  $Pd^0$  olefin products.<sup>1</sup> On the other hand, steric effects are claimed to operate in the attainment of the transition state in the hydroformylation of alkenes catalysed by  $Rh^I$ .<sup>2</sup> Of course, thermodynamic stability can accompany kinetic inertness, as found for the synthesis of L-dopa, which is governed by the different rate of  $H_2$  addition to two diastereomeric  $Rh^I$  olefin complexes.<sup>3</sup> Therefore, a correct methodology for the study of a

new ligand can not leave aside the assessment of the geometrical constraints following its coordination to the metal, from which important hints for a successful use of the ligand may be obtained.

For a long time, phosphanes have been considered as the ligands of choice for late transition metals, and they have found application in many catalytic processes. More recently, increasing attention has been directed towards nitrogen donors, which have been successfully employed in a number of asymmetric transformations.<sup>4,5</sup>

The choice of chiral N,N ligands based on natural products, i.e., carbohydrates,<sup>6–8</sup> relies on the assumption that these molecules are often easily available and may afford either lipo- or hydrosoluble ligands according to whether or not the hydroxyl groups are protected. In the latter case, the safety and economic benefit of performing the reactions in aqueous media may be added.

Previous work<sup>8</sup> described a straightforward procedure for the synthesis of  $C_2$  symmetrical chiral diimines, based on  $\alpha$ -D-glucose or  $\alpha$ -D-mannose (**1** and **2** in Fig. 1(a)). In this paper, we describe a combined synthetic, spectroscopic and crystallographic study aiming to assess the ability of ligand **1** to create an effective asym-

\* Corresponding authors. Tel.: +39-081-674460; fax: +39-081-674090.

E-mail addresses: [molinaro@unina.it](mailto:molinaro@unina.it) (A. Molinaro), [ruffo@unina.it](mailto:ruffo@unina.it) (F. Ruffo).

metric environment upon coordination to a transition-metal ion. The investigation, which has been accomplished by preparing platinum(0) complexes of general formula  $[\text{Pt}(\mathbf{1})(\text{olefin})]$ , has shown that the ligand creates a rigid and very efficient chiral pocket, which is able to recognise selectively a single enantioface of a prochiral alkene. By reacting  $[\text{Pt}(\text{norbornene})_3]$  with the equimolar amounts of chelate **1** and fumarodinitrile (fdn) in diethyl ether, complex  $[\text{Pt}(\mathbf{1})(\text{fdn})]$  (**1a**) could be isolated in high yield (Fig. 1(b)). In principle, **1a** may give rise to two diastereomers according to which enantioface of the olefin is coordinated to the metal. The  $^1\text{H}$  NMR spectrum of a fresh solution of the complex displayed both isomers in an approximate ratio of 4:1. After some minutes the ratio increased up to 98:2. This indicated that at equilibrium one of the two diastereomers is largely favoured, thus demonstrating a very high selectivity of the ligand. In order to establish the geometrical constraints, which govern this efficiency, a detailed structural investigation on compound **1a** was undertaken.

In Fig. 2 the  $^1\text{H}$  NMR and the COSY spectra of the compound in  $\text{C}_6\text{D}_6$ – $\text{CDCl}_3$  are shown (Table 1). According to the expected  $C_2$  symmetry, the two halves of both ligands are equivalent. The olefin protons are largely shifted upfield to 2.63 ppm with respect to the free unsaturated molecule in line with a large extent of  $\pi$ -back donation in the platinum–olefin bond (see below). The conformation of the nitrogen chelate is dictated by the torsional angles  $\text{H}(5)\text{--C}(5)\text{--C}(6)\text{--N}(1)$  and  $\text{C}(5)\text{--C}(6)\text{--N}(1)\text{--C}(7)$  defined as  $\psi$  and  $\phi$ , respectively (Fig. 3(a)), and by the geometry of the glucose units. Chemical shifts and coupling constants (Table 1) identify the glucose units in the expected  $^4C_1$  conformation. In order to define the  $\psi$  angle, a careful analysis of the

diastereotopic protons on C-6 was carried out. They have distinct chemical shifts and coupling constants; one appears as a triplet at  $\delta$  3.45 with  $J_{5,6R} = J_{6R,6S} = 11.7$  Hz, while the second one is a broad doublet at  $\delta$  4.17.

It is reported for the hydroxymethyl group of hexopyranoses that the dihedral angle  $\text{H}(5)\text{--C}(5)\text{--C}(6)\text{--O}(6)$  can vary around three staggered minima at:  $-60^\circ$ ,  $180^\circ$  and  $60^\circ$ , corresponding to the conformers *gauche*–*trans* (*gt*), *gauche*–*gauche* (*gg*) and *trans*–*gauche* (*tg*) respectively, and according to the assumed conformation, the NMR behaviour of the protons  $\text{H}(5)$ ,  $\text{H}(6_R)$  and  $\text{H}(6_S)$  is different as witnessed by the values of the coupling constants  $J_{5,6R}$  and  $J_{5,6S}$ . These values are described by the dihedral angle  $\text{H}(5)\text{--C}(5)\text{--C}(6)\text{--O}(6)$  according to a Karplus equation calculated on a glucose-based model.<sup>9</sup>

The compound **1a** exhibits a pattern of coupling constants diagnostic of a single staggered rotamer, the *gauche*–*trans* with  $\psi$  equal to  $-60^\circ$  (Fig. 3(b)). The presence of more conformers is excluded since the observed coupling constant values cannot be obtained by any combination of the three rotamers, while the theoretical values of the *gt* conformer are close to those measured.<sup>9,10</sup> This result is in accordance with the studies carried out on (1–6)-*O*-linked disaccharides, where it has been hypothesised that among the symmetrical orientations around the  $\text{C}(5)\text{--C}(6)$  bond (*tg*, *gt* and *gg*), the *tg* rotamer can be excluded for gluco configurations because of destabilising interactions between the equatorial oxygen at C(4) and the substituents at C(6),<sup>10</sup> whereas in this case, the *gg* rotamer can be excluded because of different values of  $J_{5,6}$ . These considerations were supported by the expected ROE effects which were observed in a 1D selective ROE. Further informa-

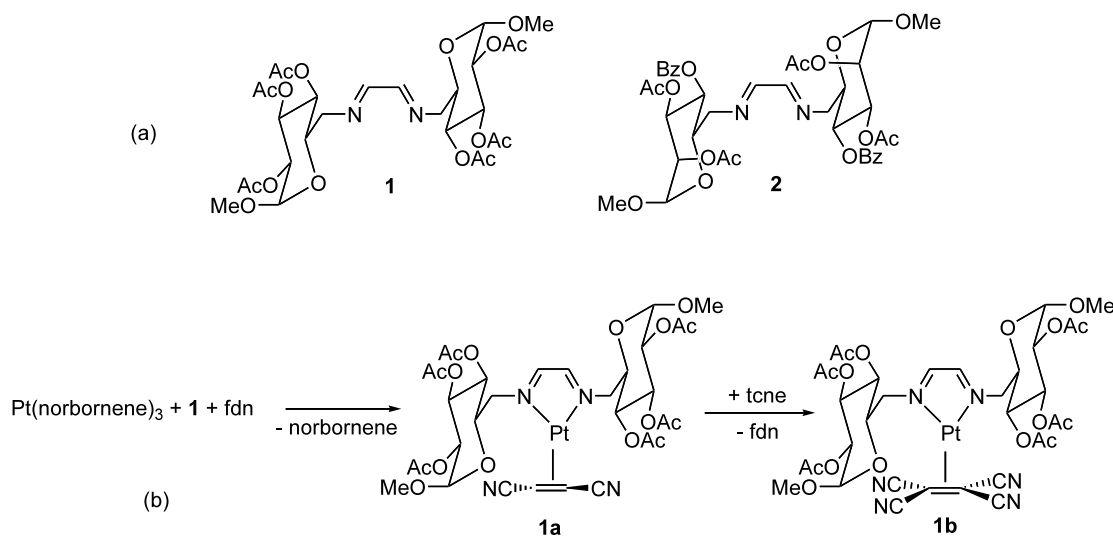


Fig. 1. (a) Two  $C_2$  symmetrical chiral diimines, based on  $\alpha$ -D-glucose (**1**) or  $\alpha$ -D-mannose (**2**); the preparation of compounds **1a** and **1b** is schematised.

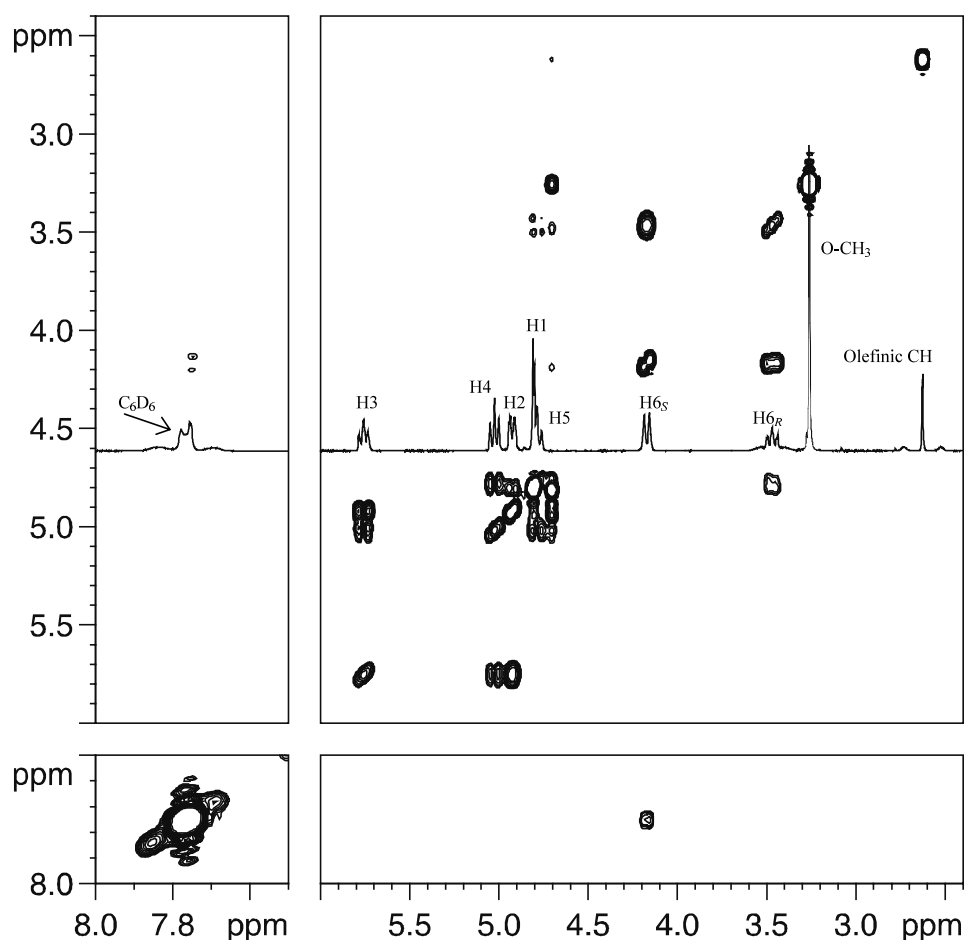


Fig. 2. Partial  $^1\text{H}$  NMR and COSY spectra of **1a**. The assignment of the sugar protons is shown along with the diagnostic correlation of the iminic proton ( $\delta$  7.76) to  $\text{H}(6_S)$ .

Table 1  
The resonances of compounds **1a** and **1b** are shown

Compound	Chemical shift										
	1	2	3	4	5	6 <sub>R</sub>	6 <sub>S</sub>	7	8	OMe	CN
<b>1a</b>											
$^1\text{H}$ ( $\text{CDCl}_3$ )	4.80	4.80	5.60	5.00	4.80	3.91	4.41	8.81	2.84	3.30	
$^1\text{H}$ ( $\text{CDCl}_3 + \text{C}_6\text{D}_6$ )	4.80	4.83	5.76	5.02	4.78	3.45	4.17	7.76	2.63	3.26	
$^{13}\text{C}$ ( $\text{CDCl}_3$ )	96.5	70.4	69.2	69.6	68.7	64.7	64.7	164.3	1.24	55.7	123.3
<b>1b</b>											
$^1\text{H}$ ( $\text{CDCl}_3$ )	4.92	4.92	5.61	5.00	4.62	4.18	4.47	8.70		3.24	

Both compounds show the usual values of coupling constants for a  $^4\text{C}_1$  conformation ( $J_{1,2} = 3$ ,  $J_{2,3} = J_{3,4} = J_{4,5} \sim 10$  Hz). The  $^{13}\text{C}$  chemical shifts of  $-\text{CO}$  groups in **1a** are at 170 ppm, whereas the  $^1\text{H}$  chemical shifts for methyl groups are at 2.01 ppm for both compounds in  $\text{CDCl}_3$ , and at 1.89 ppm for **1a** in mixture  $\text{CDCl}_3$ – $\text{C}_6\text{D}_6$ .

tion was obtained from the analysis of the COSY spectrum (Fig. 2). The signal of the iminic proton H(7) is strongly correlated only to H(6<sub>S</sub>). These protons are joined by the allylic coupling that gives a maximum coupling effect when the C(alkyl)–H bond lies in the plane of the  $\pi$ -linkage, or a minimum if such a proton is perpendicular to the same plane.<sup>11</sup> According to these considerations, the proton H(6<sub>R</sub>) must lie in the plane defined by the atoms H(7), C(7) and N(1). This restricts the values of the torsional angle  $\Phi$  to only two possibilities, i.e.,  $-110^\circ$  or  $70^\circ$ . The ambiguity is solved by means of the 1D selective ROE spectrum where a ROE effect was found between H(6<sub>R</sub>) and the iminic proton H(7) (Fig. 4) which defines unequivocally the value of  $\Phi$  to ca.  $-110^\circ$ .

Once the conformation of the nitrogen ligand is settled, it is evident that there is creation of a chiral pocket around the metal because the crowded glucose

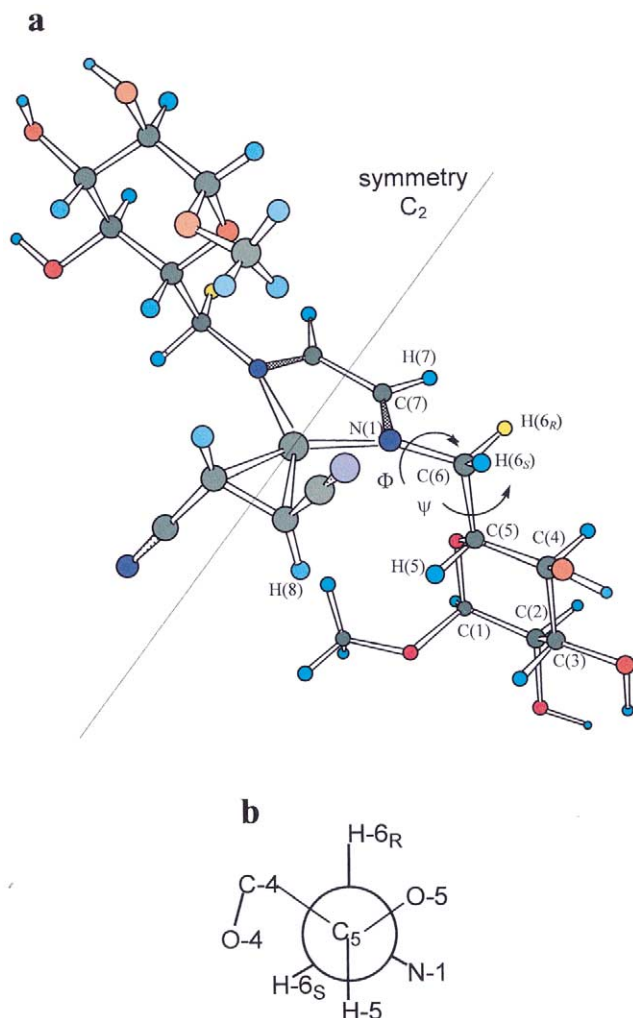


Fig. 3. (a) Ball and stick representation of **1a**, hydroxyl group must be intended as acetylated, these groups have been here omitted to avoid overcrowding of the picture; (b) the *gt* rotamer.

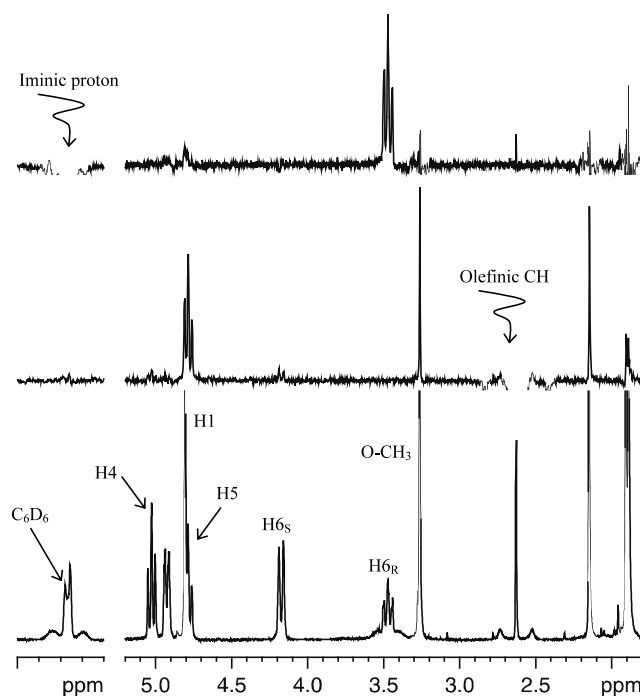


Fig. 4. (a) Section of  $^1\text{H}$  NMR spectrum of **1a**; (b) section of selective ROE spectrum obtained by saturation of the olefinic proton; (c) selective ROE spectrum saturating the iminic proton. Proton H3 is not shown in these sections.

appendages orient above and below the coordination plane on opposite sites (Fig. 3). On these grounds, the efficiency of this environment to recognise only one enantioface of fumarodinitrile can be easily predicted, as the preferred enantioface should display the  $-\text{CN}$  substituents oriented in the volume left empty by the chelate. The observation of a ROE effect between the fumarodinitrile proton and H(5) (Fig. 4) confirms this hypothesis and unequivocally assigns the orientation of the olefin as shown in Fig. 3.

In order to demonstrate that the conformation adopted by the N,N-ligand upon coordination to Pt is not induced by the olefin, the new complex **1b** was synthesised by reaction of **1a** with the highly activated tetracyanoethylene (tcne, Fig. 1(b)). The tcne substituents introduce the same type of hindrance of fdn in all of the four quadrants. Spectroscopic analysis revealed that the nitrogen chelate in **1b** assumes the same conformation in solution as found in **1a**. Proton H(6<sub>S</sub>) was correlated to the iminic proton in a COSY spectrum by the allylic coupling, whilst the H(6<sub>R</sub>) showed an ROE effect with the same proton in a ROESY spectrum. This means that the olefins have no substantial role in the conformational assessment of the ligand, which is able, by itself, to create a fairly rigid chiral pocket.

In order to ascertain whether the geometric features found in solution are retained in the solid state, single crystals of **1a** were grown. The structure of the complex

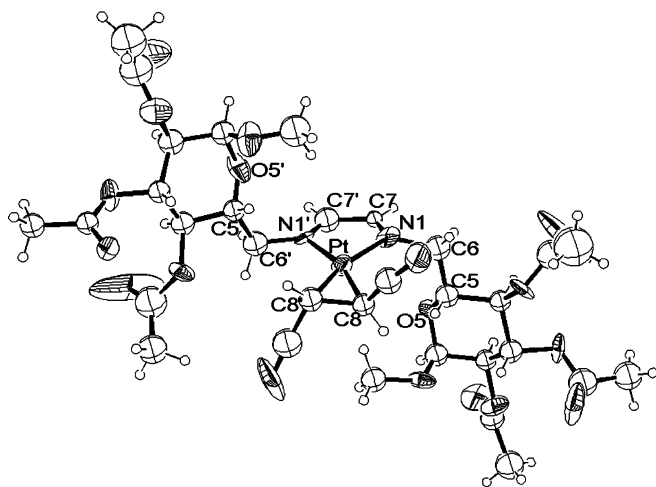


Fig. 5. ORTEP view of complex **1a** as determined through X-ray diffractometry.

was determined through X-ray diffractometry (Fig. 5, Table 2). Although the quality of diffraction data suffered owing to severe crystal degradation under X-ray beams, the solid state analysis discloses a notable agreement with the geometry found in solution. The molecule displays  $C_2$  symmetry with a planar arrangement of the coordinated atoms, as typically found in Pt(0) monoolefin compounds.<sup>12</sup> The torsional angle C(5)–C(6)–N(1)–C(7) ( $\Phi$ ) is  $-107^\circ(4)$ , in close agreement with NMR indications. The accordance holds true also for the other angle relevant for the assignment of the chelate conformation, i.e., H(5)–C(5)–C(6)–N(1) ( $\psi$ ), which is  $-66^\circ(4)$ .

As suggested by the solution study, the olefin enters the chiral pocket with a unique enantioface, in such a way as to avoid prohibitive steric contacts, especially between –CN groups and the methoxy group at C(1).

Other structural parameters worth of notice are the C=C distance [1.49(4) Å], the bending back of the carbon chain [C–C=C–C torsion angle  $38(3)^\circ$ ] and the very short Pt–N(1) [2.03(2) Å] and Pt–N(2) [2.07 (2) Å]

distances. The data indicate that a partial rehybridisation  $sp^2 \rightarrow sp^3$  of the olefin carbon atoms occurs, likely due to the presence of a consistent  $\pi$ -back donation contribution to the platinum–olefin bond. This is enhanced by the electron-withdrawing properties of the alkene and by the low charge of the metal centre, and is reinforced by a strong nitrogen-to-platinum  $\sigma$ -donation.

Thus, a combined synthetic, NMR and crystallographic investigation has demonstrated the ability of a nitrogen chelate based on glucose to create a rigid chiral pocket in trigonal Pt(0) olefin complexes. This result lies at the interface of two flourishing fields of research, as it combines the interest for N,N-chelating ligands<sup>4,5</sup> with the growing attention towards metal–sugar interactions.<sup>13</sup>

## 1. Experimental

**General methods.**—All spectra were recorded on a Bruker DRX 400 Avance spectrometer at 303 K, using a 5-mm multinuclear inverse Z-gradient-probe. One- and two-dimensional spectra (COSY, HSQC and HMB) were performed using standard pulse sequences available in the Bruker XWIN NMR 1.3 software. For 1D selective ROE and 2D COSY spectra, the sample (1 mg) was dissolved in 1:1  $C_6D_6$ – $CDCl_3$  (500  $\mu$ L). Under these conditions, the signals were not overlapping. All the heteronuclear experiments were performed in  $CDCl_3$ . Ligand **18** and  $[Pt(norbornene)_3]$ <sup>14</sup> were prepared according to literature methods. Diethyl ether was distilled from sodium immediately before use.

**Synthesis of 1a.**—To a solution of fumarodinitrile (0.15 g, 1.0 mmol) in dry  $Et_2O$  (10 mL) was added solid  $[Pt(norbornene)_3]$  (0.48 g, 1.0 mmol) in small portions. The resulting clear solution was added to a suspension of **1** (0.66 g, 1.0 mmol) in 10 mL of dry  $Et_2O$ . After 24 h of stirring, the orange precipitate was collected, washed with  $Et_2O$  ( $3 \times 5$  mL) and dried under vacuum.

Table 2  
Relevant distances (Å) and angles ( $^\circ$ ) in complex **1a**

Atom1	Atom2	Distance	Atom1	Atom2	Atom3	Angle	Atom1	Atom2	Atom3	Atom4	Angle
Pt	N1	2.05(3)	N1	Pt	C8	120(1)	H5	C5	C6	N1	$-66(4)$
Pt	C8	2.00(3)	N1	Pt	C8'	164(1)	C7	N1	C6	C5	$-107(4)$
N1	C6	1.52(5)	N1	Pt	N1'	74(1)					
N1	C7	1.25(4)	N1'	C6'	C5'	106(3)					
C8	C8'	1.51(5)	N1'	Pt	C8'	122(1)					
Pt	N1'	2.11(2)	N1'	Pt	C8	164(1)					
Pt	C8'	2.03(3)	C8	Pt	C8'	44(1)					
N1'	C6'	1.46(5)	N1	C6	C5	112(3)					
N1'	C7'	1.20(5)									

Numbers in parentheses are estimated in standard deviations in the last significant digits.

The product could be purified by chromatography on silica gel with 40:1  $\text{CH}_2\text{Cl}_2$ –MeOH. The solvents were removed under vacuum from the collected orange fractions, affording the product as a red microcrystalline solid (yield 85%). Anal. Calcd for  $\text{C}_{32}\text{H}_{42}\text{N}_4\text{O}_{16}\text{Pt}$ : C, 41.16; H, 4.53; N, 6.00. Found: C, 41.34; H, 4.45; N, 5.89.

**Synthesis of 1b.**—To a solution of **1a** (0.10 g, 0.010 mmol) in  $\text{CH}_2\text{Cl}_2$  (5 mL) was added solid tetracyanoethylene (0.015 g, 0.11 mmol). After 12 h of stirring, the solvent was removed under vacuum, and the resulting red powder washed several times with  $\text{Et}_2\text{O}$  and dried. Yield was almost quantitative. Anal. Calcd for  $\text{C}_{34}\text{H}_{40}\text{N}_6\text{O}_{16}\text{Pt}$ : C, 41.51; H, 4.10; N, 8.54. Found: C, 41.65; H, 4.01; N, 8.70.

**Experimental details of X-ray data collection.**—The compound was recrystallised from  $\text{CH}_2\text{Cl}_2$ –hexane. A single-crystal of suitable size ( $0.05 \times 0.2 \times 0.4$  mm) was examined. The unit cell parameters were obtained by a least-squares fitting of the setting values of 25 reflections in  $\theta$  range  $11 \leq \theta \leq 13^\circ$ . Crystal data:  $\text{C}_{32}\text{H}_{42}\text{N}_4\text{O}_{16}\text{Pt}$ ,  $f_w = 933.80 \text{ g mol}^{-1}$ , orthorhombic,  $P2_12_12_1$  [ $a = 11.382(6)$ ,  $b = 17.696(8)$ ,  $c = 21.883(9) \text{ \AA}$ ,  $V = 44076(5) \text{ \AA}^3$ ,  $Z = 4$ ,  $D_{\text{calcd}} = 1.40 \text{ g cm}^{-3}$ ]. X-ray data were collected at rt on an Enraf–Nonius CAD4-F automatic diffractometer using Mo  $\text{K}_\alpha$  graphite-monochromated radiation ( $\lambda_{\text{Mo K}_\alpha} = 0.71073 \text{ \AA}$ ) and operating in the  $\omega/\theta$  scan mode,  $2\theta_{\text{max}} = 54^\circ$ , number of independent reflections 5325. Three monitoring reflections measured every 500, showed an intensity decay of about 37% for which a linear correction was applied. In addition to the corrections for Lorentz and polarization factors, an empirical correction for absorption based on Fourier analysis of data was applied (max and min values of the transmission factor were 1.4 and 0.3). The structure was solved by direct-methods (Multan) and Fourier techniques and refined by full-matrix least-square procedure minimising the quantity  $\sum w(|F_o| - |F_c|)^2$  with  $w^{-1} = [\sigma^2(F_o) + (0.02F_o)^2 + 1]$  where  $\sigma$  is derived by counting statistics. All non-hydrogen atoms, but carbon atoms, were refined anisotropically. The H atoms were placed in calculated positions and are included but not refined in last-refinement cycles with isotropic thermal parameters equal to those of the carrier atoms. The final Fourier difference

map showed no peaks greater than  $1.3 \text{ e \AA}^{-3}$ . The final structure, with  $R = 0.074$  and  $R_w = 0.094$ , was obtained from the 2100 reflections with  $F_o > 3\sigma F_o$ ) and 318 independent parameters.

All calculations were performed by using the Enraf–Nonius SDP set of programs.<sup>15</sup>

## Acknowledgements

The authors thank the Consiglio Nazionale delle Ricerche, the MURST (Programmi di Ricerca Scientifica di Rilevante Interesse Nazionale, Cofinanziamento 2000–2001), and the Centro Interdipartimentale di Metodologie Chimico-Fisiche, Università di Napoli ‘Federico II’ for NMR and X-ray facilities.

## References

1. Pfaltz, A. In *Advances in Catalytic Processes*; Doyle, M. P., Ed.; Jai Press: London, 1995; Vol. 1, pp. 61–94.
2. Stanley, G. G. In *Advances in Catalytic Processes*; Doyle, M. P., Ed.; Jai Press: London, 1997; Vol. 2, pp. 221–243.
3. Knowles, W. S. *Acc. Chem. Res.* **1983**, *16*, 106–112.
4. Fache, F.; Schulz, E.; Tommasino, M. L.; Lemaire, M. *Chem. Rev.* **2000**, *100*, 2159–2232.
5. Togni, A.; Venanzi, L. M. *Angew. Chem., Int. Ed. Engl.* **1994**, *33*, 517–547.
6. Borriello, C.; Cucciolito, M. E.; Panunzi, A.; Ruffo, F. *Tetrahedron: Asymmetry* **2001**, *12/17*, 2467–2471.
7. Borriello, C.; Ferrara, M. L.; Orabona, I.; Panunzi, A.; Ruffo, F. *J. Chem. Soc., Dalton Trans.* **2000**, 2545–2550.
8. Ferrara, M. L.; Giordano, F.; Orabona, I.; Panunzi, A.; Ruffo, F. *Eur. J. Inorg. Chem.* **1999**, 1939–1947.
9. Homans, S. W.; Dwek, R. A.; Boyd, J.; Mahmoudian, M.; Richards, W. G.; Rademacher, T. W. *Biochemistry* **1986**, *25*, 6342–6350.
10. Bock, B.; Duus, J.Ø. *J. Carbohydr. Chem.* **1994**, *13*, 513–543.
11. Friebolin, H. *Basic One- and Two-Dimensional NMR Spectroscopy*; VCH: Weinheim, 1991; p. 84.
12. Albano, V. G.; Castellari, C.; Monari, M.; De Felice, V.; Panunzi, A.; Ruffo, F. *Organometallics* **1996**, *15*, 4012–4019.
13. Steinborn, D.; Junicke, H. *Chem. Rev.* **2000**, *100*, 4283–4318.
14. Craswell, L. E.; Spencer, J. L. *Inorg. Synth.* **1990**, *28*, 126–128.
15. Frenz, B. *Crystallographic Computing 5*; Oxford University Press: Oxford, 1991; p. 11, 126.